This is a repository copy of *Investigation of wrinkling initiation in shear spinning*.

White Rose Research Online URL for this paper:
https://eprints.whiterose.ac.uk/226638/

Version: Published Version

Proceedings Paper:
Li, Z. and Long, H. orcid.org/0000-0003-1673-1193 (2025) Investigation of wrinkling initiation in shear spinning. In: Martins, P.A.F., Santos, A.D. and Oliveira, M.C., (eds.) MATEC Web of Conferences. 44th Conference of the International Deep Drawing Research Group (IDDRG 2025), 01-05 Jun 2025, Lisbon, Portugal. EDP Sciences

https://doi.org/10.1051/matecconf/202540801040

Reuse
This article is distributed under the terms of the Creative Commons Attribution (CC BY) licence. This licence allows you to distribute, remix, tweak, and build upon the work, even commercially, as long as you credit the authors for the original work. More information and the full terms of the licence here: https://creativecommons.org/licenses/

Takedown
If you consider content in White Rose Research Online to be in breach of UK law, please notify us by emailing eprints@whiterose.ac.uk including the URL of the record and the reason for the withdrawal request.

eprints@whiterose.ac.uk
https://eprints.whiterose.ac.uk/

Investigation of Wrinkling Initiation in Shear Spinning

Zhikun Li[1], and *Hui* Long[1*]

[1]The University of Sheffield, School of Mechanical, Aerospace and Civil Engineering, Sheffield, S1 3JD, United Kingdom

Abstract. Metal spinning is a flexible and net-shape sheet forming process however its process development still heavily relies on empirical knowledge to determine process parameters to avoid processing failures, such as wrinkling. This paper develops dynamic finite element modelling of a shear spinning process to investigate wrinkling initiation and critical strains leading to wrinkling. Two processing parameters, mandrel rotational speed and roller feed rate, in spinning aluminium sheet material AA5251-H22 are investigated to ascertain the effect of the roller feed ratio on wrinkling, validated by a spinning experiment. The evolution of the maximum circumferential and radial strains on the top surface of wrinkling waves is evaluated and it has been found that they accumulate progressively with the formation of wrinkling. The wrinkling initiates when the maximum circumferential strain of the top surface of winkling waves cyclically increases and remains tensile. The FE results indicate that the dynamic effect due to a higher mandrel speed, thus a greater strain rate, is independent of the wrinkling initiation providing that the roller feed ratio remains unchanged and below a certain limit. The wrinkling initiation is the result of the circumferential strain accumulation when the roller feed ratio applied to the sheet exceeds a limit.

Keywords: Metal spinning; Wrinkling; Finite element modelling; Strain analysis.

1 Introduction

Metal spinning process has advantages of process flexibility and net-shape manufacturing. By employing spinning, the material formability is also improved due to the localised material deformation under cyclic loading. The high material utilisation and forming accuracy of metal spinning benefit small batch and customised product manufacturing in various industrial applications. However, the design of the metal spinning process still heavily relies on empirical knowledge to avoid process failures, in which wrinkling failure occurs most often. There is no established industrial standard or design methods to determine the processing parameters to prevent wrinkling failure in the spinning process. Material deformation and the effect of strain evolution on wrinkling initiation are not clear. Trial-and-error and preliminary tests are commonly used in developing the spinning process for a new product or using a new material. This significantly compromises the production efficiency and product repeatability, and causes material, operator and machine time wastes.

During spinning, a sheet metal blank is deformed by a roller into an axisymmetric shape of a component; single or multiple roller paths may be required, as illustrated in Fig.1. The sheet material is subjected to multiaxial deformation under dynamic conditions due to the action of the roller, including tension, bending, shearing, and cyclic loading. Wrinkling usually occurs in the un-spun flange of the workpiece during the process, and it becomes more severe while the roller continues to deform the workpiece [2]. To understand the material stress and strain distribution and evolution during spinning, both experimental measurements and finite element modelling methods are developed. The plugged hole method was developed by Avitzur and Yang [3], while the grid line method was used by Kalpakcioglu [4]. The grid etching method was developed by Quigley and Monaghan [5] and also employed by Beni et al. [6]. The material deformation modes at different locations of the spun workpiece were evaluated. Although some of these methods were able to obtain strain results, the accuracy of strain measurements was not acceptable. Finite element (FE) modelling of spinning processes has been increasingly reported to investigate material deformation, wrinkling failure and effects of process parameters by combining FE modelling and the design of experiment methods [7, 8]. Both shearing and bending deformation modes were identified as important factors to initiate wrinkling while employing a higher roller feed ratio resulted in wrinkling to occur more earlier in the process.

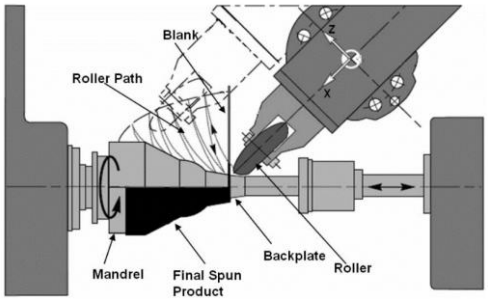

Fig. 1. Illustration of multi-pass metal spinning [1]

* Corresponding author: h.long@sheffield.ac.uk

© The Authors, published by EDP Sciences. This is an open access article distributed under the terms of the Creative Commons Attribution License 4.0 (https://creativecommons.org/licenses/by/4.0/).

As spinning is a highly dynamic process, the study into the dynamic instability during spinning was reported by developing analytical and experimental methods [9, 10]. However these methods were unable to quantify stress and strain values and their distribution and evolution to predict the wrinkling initiation. Two recent studies [11, 12] developed methods to predict wrinkling initiation considering the effects of various spinning process parameters; however the evolution of critical strains during spinning was not investigated.

This paper presents the development of a dynamic finite element (FE) modelling of a shear spinning process and detailed analysis of wrinkling formation and evolution of critical strains. The primary focus is to investigate the causes of wrinkling occurrence regarding the material deformation during wrinkling formation. The effect of the process dynamics and strain rate is investigated by varying the mandrel rotational speed and roller feed rate proportionally to keep the roller feed ratio unchanged.

2 Methods and procedures

Both FE analysis and experimental testing of a shear spinning process are conducted. The spinning process parameters are selected to cause wrinkling thus its initiation and propagation can be analysed. Two FE models of the shear spinning process by using ABAQUS/Explicit are developed to obtain the strain and stress results under different processing conditions, as shown in Table 1, Figs.2 and 3. The continuum shell element, SC8R, is selected for the sheet workpiece. Each element has eight nodes and is quadrilateral using first-order interpolation to calculate stresses and displacements with reduced integration. Compared with conventional shell elements, the SC8R element can model problems with complex contact conditions and most critically, consider transverse shear deformation. Through the sheet thickness of 1mm, there are nine integration points to model bending deformation accurately. The roller, backplate and mandrel are simulated as rigid bodies. Frictional coefficient for each contact surface is defined, 0.5 for backplate-workpiece and mandrel-workpiece, and 0.02 for roller-workpiece.

To validate FE modelling results of wrinkling, the experiment of the shear spinning, as shown in Fig.3, Test 1 and 2 are conducted under the same conditions as that of the FE models. Vibrations are generated when the roller works over the workpiece due to the direct contact between roller and workpiece surfaces. Vibrations become greater when wrinkling on the workpiece surface occurs thus the wrinkling initiation time can be detected. The number of wrinkling waves and wrinkling amplitudes can be obtained from a tested workpiece to compare with the FE modelling results.

Two different mandrel rotational speeds are tested, as shown in Table 1, but the roller feed ratio is kept the same by varying the roller feed rate proportionally. This is to investigate if the feed rate or strain rate influences the initiation and severity of wrinkling, while the feed ratio remains unchanged. The feed ratio and processing time can be calculated by Eq.(1), (2) respectively. For Model 1, the processing time is only one fifth of that Model 2, due to a higher roller feed rate of the latter.

$$feed\ ratio\ (mm/rev) = \frac{feed\ rate\ (mm/s)}{mandrel\ speed\ (rev/s)} \quad (1)$$

$$processing\ time\ (s) = \frac{roller\ moving\ distance\ (mm)}{feed\ rate\ (mm/s)} \quad (2)$$

Table 1. Spinning process parameters, material AA5251-H22

Workpiece radius	Workpiece thickness	Thickness reduction	Clearance
70 mm	1 mm	0.29 mm	0.71 mm
Model 1 / Test 1		Model 2 / Test 2	
Feed ratio: 1.5 mm/rev	Processing time: 2.16 s	Feed ratio: 1.5 mm/rev	Processing time: 10.8 s
Feed rate: 52.36 mm/s		Feed rate: 6.98 mm/s	
Mandrel rotational speed: 1000 rpm		Mandrel rotational speed: 200 rpm	
Density: 2690 kg/m^3	Young's modulus: 69 GPa		Poisson's ratio: 0.3

3 Results and discussion

3.1 Wrinkling wave amplitude

Fig.2 shows the wrinkling development at six different stages during the spinning process under the mandrel speed of 1000 rpm (Model 1). Terms of wrinkling wave amplitude, wrinkling top and bottom surfaces are introduced to analyse the FE modelling results and compare with the experiment, as shown in Fig.4. Normalised circumference of the workpiece is used in the result analysis for easy comparison.

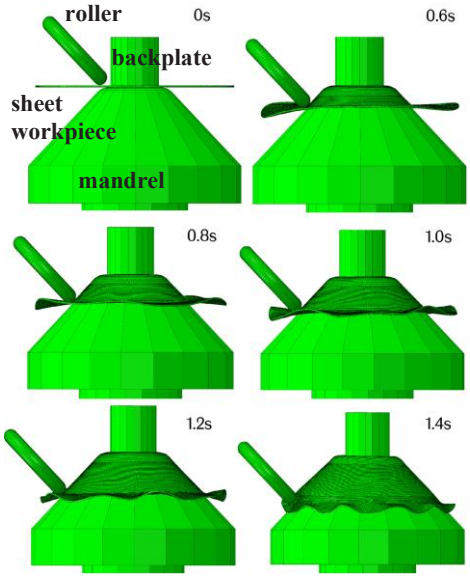

Fig. 2. Modelling of wrinkling in shear spinning (Model 1)

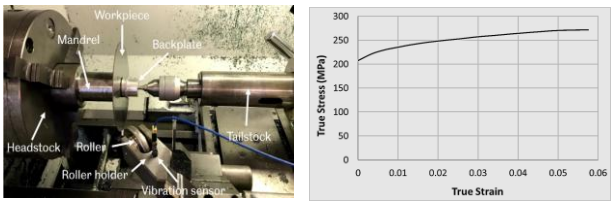

Fig. 3. Roller vibration measurement and sheet flow stress

Fig.5 shows an increasing trend of the wrinkling wave amplitude while the spinning process progresses at five different times (or mandrel rotations). Comparing FE Model 2 and Test 2 in Fig.6, it shows that wrinkling amplitudes are very close; and FE model and experiment generate the same number of the wrinkling waves.

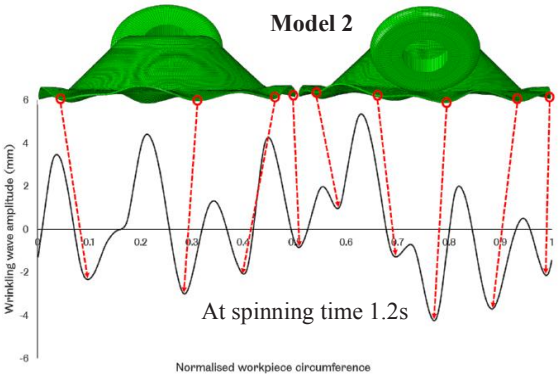

Fig. 4. Illustration of wrinkling wave top and bottom (Model 2)

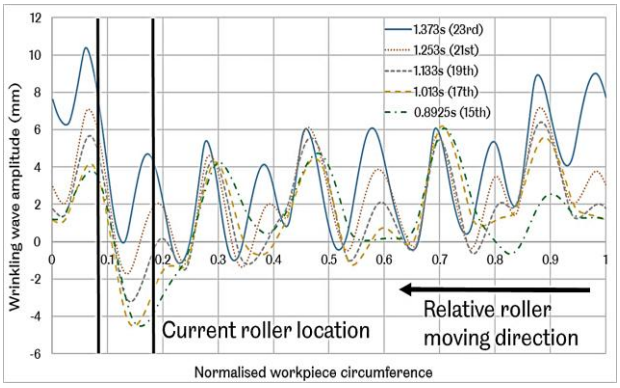

Fig. 5. Wrinkling wave amplitudes at different times (Model 1)

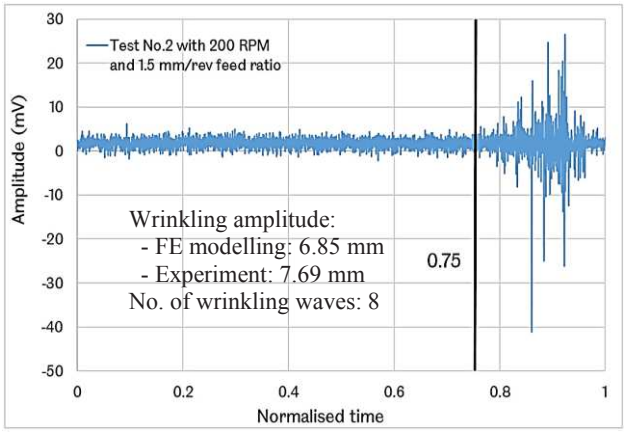

Fig. 6. Experimental measured wave forms of Test 2 and comparison of wrinkling wave amplitudes of Model 2 & Test 2

3.2 Effect of mandrel speed on wrinkling

To ascertain the mandrel rotational speed or strain rate would not affect the occurrence of wrinkling, Fig.7 compares the edge heights of the workpiece circumference of Models 1 and 2. Even though spun under different mandrel speed, the wrinkling edge heights of the workpieces are very similar. The wrinkling waves and severity, shown in Fig.8, in both models are also very similar at the equivalent stage of the spinning process, at 1.43s for Model 1 and 7.17s for Model 2. Both FE and experimental results show that the wrinkling initiation and wrinkling amplitude are not affected by the dynamic effect or strain rate induced by applying different mandrel speeds or roller feed rates, providing that the feed ratio remains unchanged. However, the vibration waveform results measured from the experiment also indicate that the roller vibration is less severe for tests under a relatively lower mandrel rotational speed.

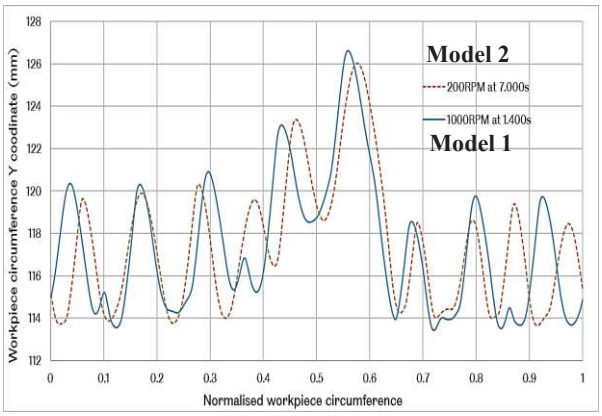

Fig. 7. Comparison of wrinkling heights and effect of feed rate

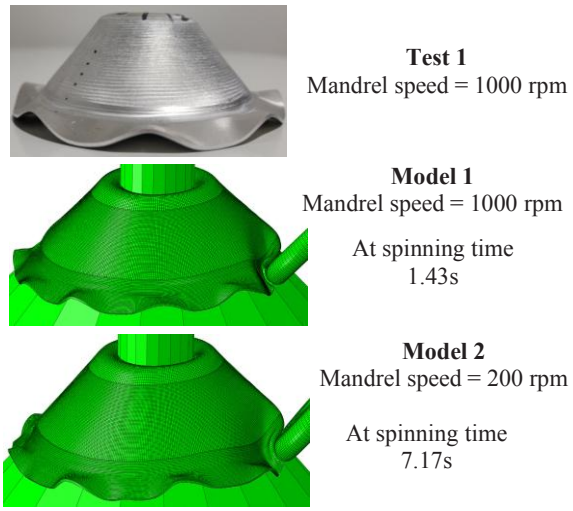

Fig. 8. Comparison of wrinkling severity and effect of feed rate

3.3 Strain analysis of wrinkling initiation

To investigate the wrinkling initiation, critical locations of the workpiece need to be identified first before detailed strain analysis. Because the location of the most severely wrinkled region of the workpiece is constantly changing during spinning, the material on the wrinkling top line with the greatest wrinkling amplitude is initially considered to be the most severely wrinkled location. However, it has been observed that the wrinkling top line does not coincide with the location of the maximum circumferential strain, as shown in the strain contour plot in Fig.9. As a result, the location of the maximum circumferential strain is used for the following strain analysis of wrinkling initiation by selecting a total of 14 FE nodes on the wrinkling top surface, shown in Fig.9.

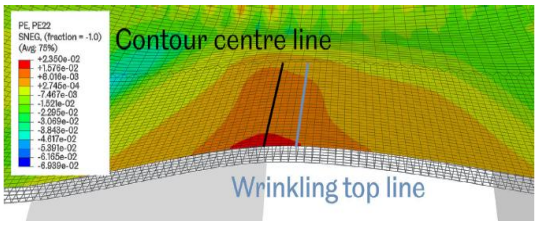

Model 1 at spinning time 0.8925s

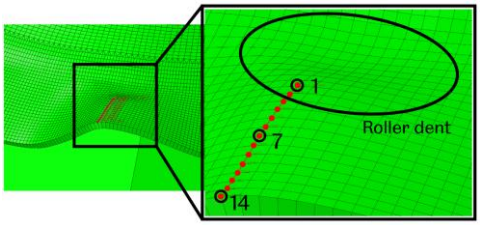

Model 1 at spinning time 1.735s

Fig. 9. Locations of wrinkling top and maximum strain line

In the earlier stage of the spinning process, the circumferential and radial strains on the top surface of a wrinkled workpiece are very small and barely any wrinkling wave is noticeable. The strain diagram is drawn with the maximum circumferential strain as major strain and the radial strain as minor strain. Fig.10 shows the distribution and evolution of the maximum circumferential and radial strains of the wrinkling top surface. The maximum circumferential and radial strains of the 14 selected nodes on the wrinkling top surface, at different times during the spinning process, from 0.7725s (13th mandrel revolution) to 1.373s (23rd mandrel revolution) for FE Model 1, from 4.3s (14th mandrel revolution) to 7.0s (23rd mandrel revolution) for FE Model 2, are shown in Fig.10. The maximum circumferential and radial strains are very small at the early stage of the spinning process, but the strains increase and expand to a wider space on the strain diagram after each mandrel revolution because the workpiece material is continued to be worked on by the roller.

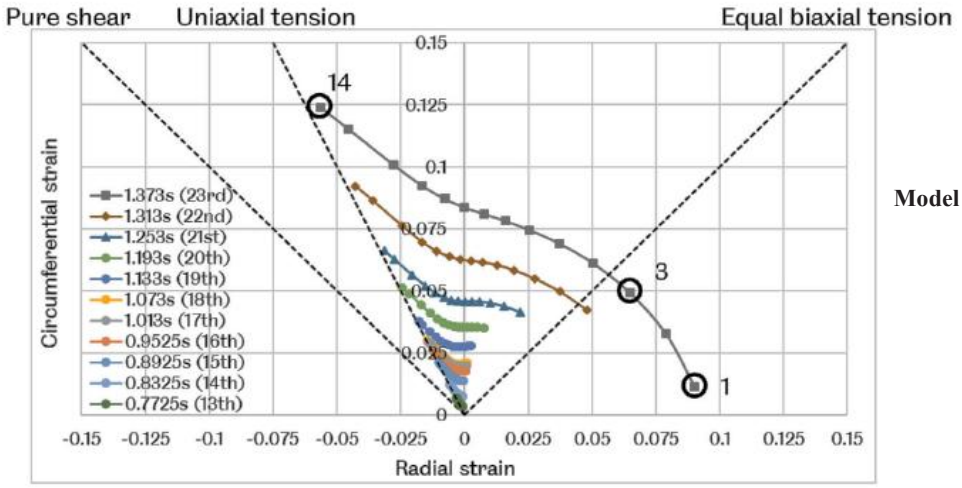

Model 1

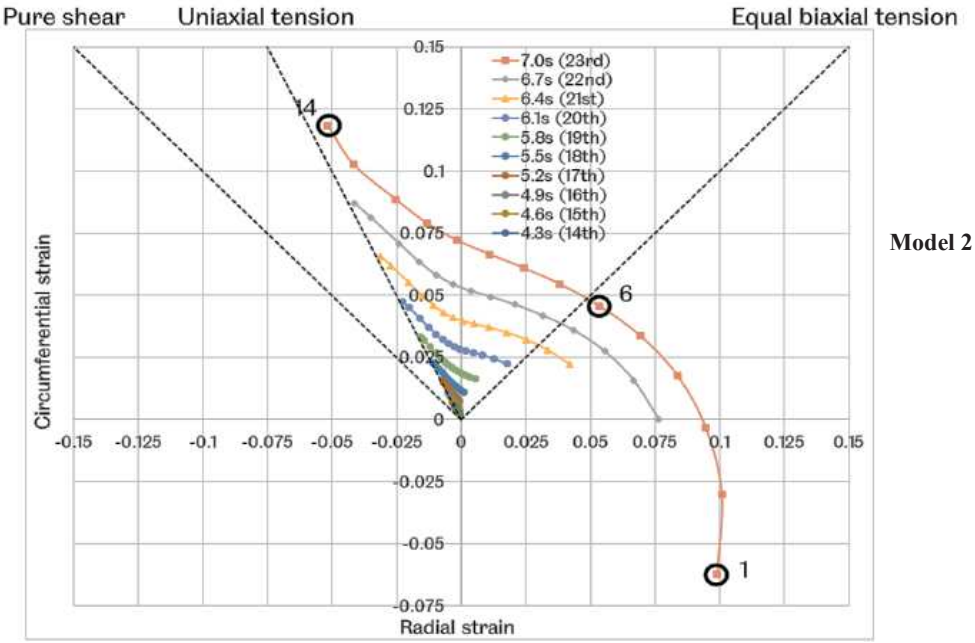

Model 2

Fig. 10. Evolution of maximum circumferential and radial strains on wrinkled top surface

There is an obvious pattern that both maximum circumferential and radial strains on the wrinkling top surface increase continuously as the spinning proceeds when the roller deforms the material of the workpiece gradually. Fig.11 shows the ratio of the radial strain (RS) to the circumferential strain (CS) of the wrinkling top and bottom surfaces of Model 1. It is clear there is a linear relationship between the two strains, from the beginning to reach the greatest strain values at 1.373s when the FE mesh of the workpiece is significantly distorted due to severe wrinkling.

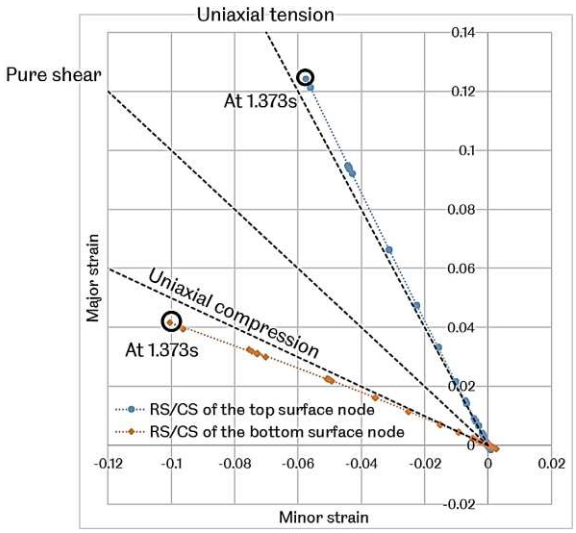

Fig.11 Ratio of radial and circumferential strain of Model 1

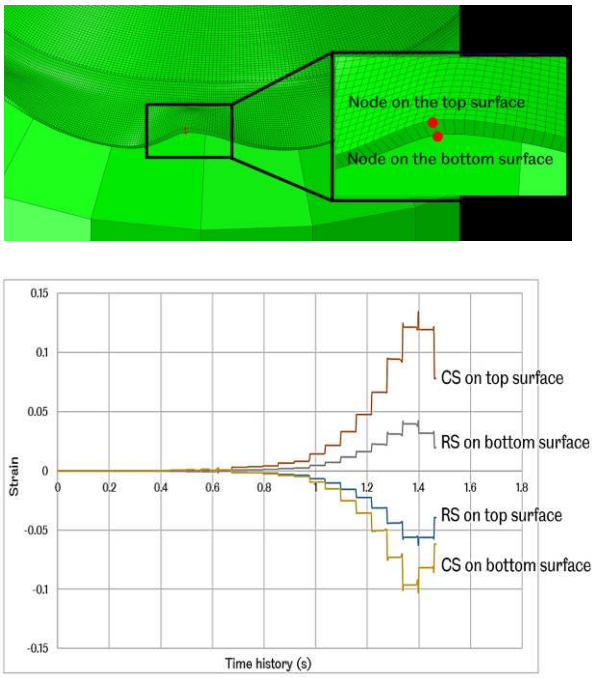

Fig. 12. Time history of strains on wrinkle top and bottom surfaces

As shown in Fig.10, from the 13rd mandrel revolution, the strains induced by the roller became greater and greater after each mandrel revolution. The strains accumulate and cyclically increase while the spinning process continues. Fig.12 shows the time history of the maximum circumferential strain (CS) and radial strain (RS) of both top and bottom surfaces of the wrinkled wave of the workpiece. The positive values of the circumferential strain on the top surface is a result of the formation of the wrinkling wave, acting as plastic bending deformation of the workpiece flange, inducing tension of the top surface and compression of the bottom surface of the wrinkling wave in the circumferential direction, as illustrated in Fig.13.

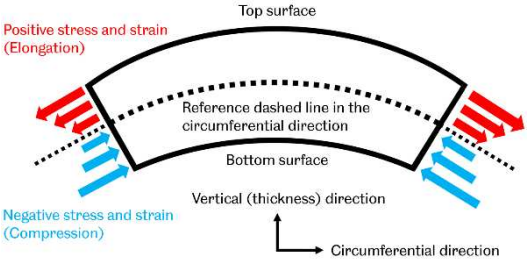

Fig. 13. Tensile and compressive strains of wrinkling wave

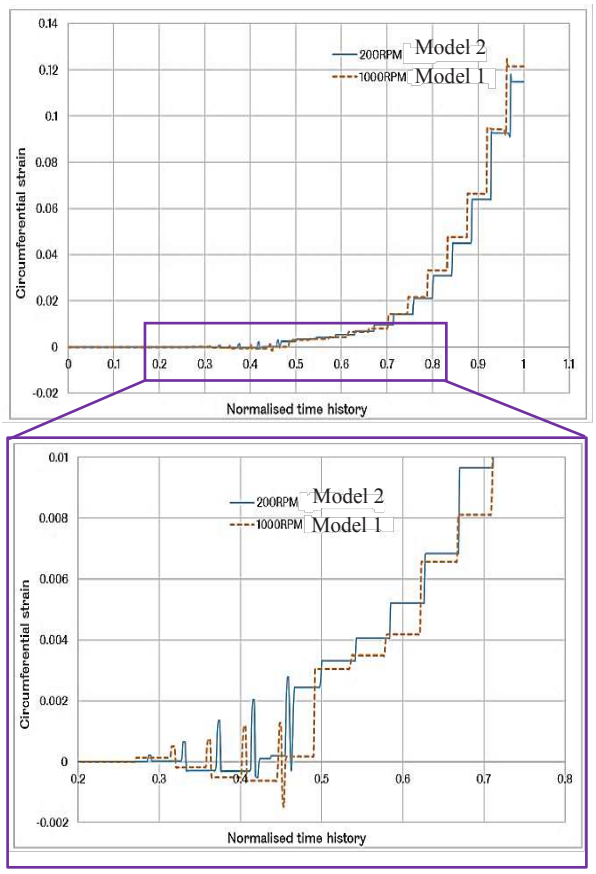

Fig. 14. Time history of circumferential strain of Models 1 and 2

Fig.14 compares the maximum circumferential strains of the top surface of FE Models 1 and 2. Due to the difference of the mandrel rotational speed and roller feed rate, the spinning time of each of these spinning processes are different, as shown in Table 1. In order to compare the strain results and evaluate the effect of strain rate on wrinkling initiation, the normalised time history is used to present the maximum circumferential strain results. The strain history results of two FE Models have very similar patterns, under the mandrel speed of 1000 rpm for Model 1 and 200 rpm for Model 2. The detailed strain results from 0.2 to 0.8 of the normalised time are shown in an enlarged view in Fig.14. Between 0.3~0.5 of the

normalised time, it can be seen that the circumferential strain keeps a slightly increasing trend to very small positive values, indicating that the top surface is slightly elongated after the roller works over the nearby material. The strain reduces immediately after the roller moves away from the area. The strain reduces to a negative value but is very close to zero, indicating that the top surface is slightly compressed. During this time period, the material of the top surface can recover from the deformation, induced by the roller, to maintain a small negative value of the circumferential strain.

In the early stage of the spinning process, the roller travels a shorter distance on the flange of the workpiece to complete one revolution, while a greater flange width provides sufficient stiffness of the workpiece to resist wrinkling. The flange width of the workpiece gradually reduces as the roller deforms the flange material progressively and moves outward from the centre to the edge of the workpiece, significantly increasing the wrinkling risk. As shown in Fig.14, after 0.45 of the normalised time, the maximum circumferential strain induced by the roller becomes greater and greater. The positive circumferential strain on the top surface accumulates after each roller contact with the workpiece, leading to the wrinkling failure.

As can be seen in Fig.14, the normalised time of the start of the circumferential strain accumulation for FE Models 1 and 2 is the same; and the circumferential strain values themselves are also similar; showing that the dynamic effect or strain rate in spinning, due to different mandrel rotational speed or roller feed rate, does not affect the wrinkling initiation, as long as the feed ratio is kept unchanged. For both FE models, the feed ratio is the same, equal to 1.5mm/rev, but the roller deforms the workpiece five times faster in FE Model 1 than that in FE Model 2. The analysis of the strain results further prove that even with a five-time difference in deformation speed of the material, the feed ratio is the most critical factor that affects the wrinkling initiation and strain accumulation in the spinning process, not the effect of the dynamic deformation or strain rate. The wrinkling initiation is the result of the accumulation of the maximum circumferential strain when the roller feed ratio applied to the sheet exceeds a limit.

4 Conclusions

This paper develops a dynamic FE modelling of a shear spinning process to investigate wrinkling initiation and critical strains leading to wrinkling failure. The dynamic effect or strain rate effect on wrinkling in spinning is evaluated by varying the mandrel rotational speed and roller feed rate proportionally, to keep the roller feed ratio unchanged. Based on the results obtained, the following conclusions can be drawn:

- The maximum circumferential strain on the top surface of wrinkling waves is critical for the initiation of wrinkling in spinning. The wrinkling initiates when the maximum circumferential strain accumulates and cyclically increases, and remains tensile. The maximum circumferential strain remains compressive while the workpiece flange is wrinkling-free at the early stage of the spinning process.
- The wrinkling wave amplitude is proposed to quantify the severity of the wrinkling formation in this study. It has shown that it increases with the severity of the wrinkling waves of the workpiece flange. The FE modelled and experimental measured results of the wrinkling wave amplitude are similar. However, both the wrinkling wave amplitude and the maximum circumferential strain at the early stage of spinning with minor wrinkling are difficult to measure because they are both very small.
- The FE strain analysis and experimental test results of the spinning process indicate that the dynamic or strain rate effect, due to a high mandrel speed or greater roller feed rate, does not affect the wrinkling initiation and severity of the wrinkling, providing that the roller feed ratio is kept constant and below a certain limit. The wrinkling initiation is the result of the maximum circumferential strain accumulation due to an excessive feed ratio applied to the workpiece material by the roller during the spinning process.

Acknowledgements

The authors would like to acknowledge the financial support received from the UK Engineering and Physical Sciences Research Council (EPSRC) through project grants EP/W010089/1 and EP/T005254/1.

References

1. M. Runge, *Spinning and Flow Forming* (Leifeld GmbH, 1994)
2. O. Music, J. M. Allwood, K. Kawai, J. Mater. Process. Technol., **210**, 1 (2010)
3. B. Avitzur and C. T. Yang, J. Eng. Ind., **82**, 3 (1960)
4. S. Kalpakcioglu, J. Manuf. Sci. Eng. Trans. ASME, **83**, 2 (1961)
5. E. Quigley and J. Monaghan, J. Mater. Process. Technol., **121**, 1 (2002)
6. H. R. Beni, Y. T. Beni, and F. R. Biglari, In Proc. Inst. Mech. Eng. Part C J. Mech. Eng. Sci., **225**, 3 (2011)
7. L. Wang, H. Long, Materials and Design, **32.** 5 (2011)
8. M. Watson, H. Long, B. Lu, Int. J. Adv. Manuf. Technol., **78**, 981-995 (2015)
9. S. Kobayashi, J. Manuf. Sci. Eng. Trans. ASME, **85**, 1 (1963)
10. M. Kleiner, R. Göbel, H. Kantz, C. Klimmek, W. Homberg, CIRP Ann. - Manuf. Technol., **51**, 1 (2002)
11. T. Childerhouse, H. Long, Procedia Manuf., **29** (2019)
12. Z.H. Li, H. Long, J. Mater. Process. Technol., **300**. 117399 (2022)